ISSN (Print) 1226-1750
ISSN (Online) 2233-6656
Journal of Magnetics 18(4), 443-453 (2013) http://dx.doi.org/10.4283/JMAG.2013.18.4.443

Research on Forces and Dynamics of Maglev Wind Turbine Generator

Nianxian Wang*, Yefa Hu, Huachun Wu, Jinguang Zhang, and Chunsheng Song

School of Mechanical and Electronic Engineering, Wuhan University of Technology, Wuhan 430070, China

(Received 26 February 2013, Received in final form 13 August 2013, Accepted 14 October 2013)

Maglev wind turbine generator (MWTG) technology has been widely studied due to its low loss, low maintenance cost, and high reliability. However, the dynamics of the magnetic bearing system differ fromthe those of the traditional mechanical bearing system. A horizontal axial MWTG supported with a permanent magnetic bearing is designed in this research and the radial forces and the natural frequencies of the rotor system are studied. The results show that the generatorhas a cyclical magnetic forceand an unreasonable bearing stiffness may mean that the rotor system needs to work in the resonance region; the bearing stiffness is the key factor to avoid this problem. This is the main rule of the bearing stiffness design in the MWTG, and this rule can also be used in other maglev permanent magnet motors.

Keywords : wind turbine generator, permanent magnetic bearings, magnetic forces, bearing stiffness, natural frequency

1. Introduction

The development of wind power is important to solve the problem of energy shortage and reduce the emission of greenhouse gases. Currently, wind turbine generators are mainly supported by traditional mechanical bearings. However, wind turbine generators work in harsh environments with excessively large dynamic loads, and the mechanical bearings need to be lubricated and maintained constantly. This increases the cost of wind power significantly; moreover, the friction of mechanical bearings reduces the overall efficiency of the drive train.

Magnetic bearings have no friction, no wearing, and no lubrication [1]. The mechanical wear of bearings can be completely eliminated by using magnetic bearings in wind turbine generators. Efficiency and reliability will also improve in a maglev wind turbine generator (MWTG).

The MWTG has been studied by many researchers. G. Shrestha used the magnetic bearings in a horizontal axis direct-drive wind turbine generator in [2] and [3]. A magnetic bearing based on the rotor system in a 5 MW wind turbine generator is designed, and the performance is compared with the traditional bearings. The result shows that, while the power losses are the same, the mass of the wind turbine generator is reduced significantly. N. C. Tsai and H. Wu show the application of magnetic bearings in vehicle wind turbine generators in [4] and [5]. Active magnetic bearings have been used and the control systems of active magnetic bearings have been studied. S. Liu designed a maglev vehicle wind turbine generator, and the research showed that the wind turbine generator with magnetic bearing is more efficient [6]. Y. H. Fan designed a passive magnetic trust bearing for a small vehicle wind generator system and experiment results showed that this system can start at a lower wind speed and can increase in efficiency by 20%-50% [7].

Current research on MWTG shows that wind turbine generators with magnetic bearings have a lower mass, higher efficiency, and higher reliability than traditional wind turbine generators.

Three types of magnetic bearings are typically used: permanent magnetic bearings (PMB), active magnetic bearings (AMB), and hybrid magnetic bearings (HMB). Compared with other types of magnetic bearings, PMB has the advantages of not needing to be controlled, a low cost, a simple structure, and no response time [1]. PMB is therefore more suitable for a wind turbine generator [8].

However, PMB and mechanical bearings differ significantly. The stiffness of PMB is small and the air gap between the rotor and stator is considerable, whereby the center of the rotor is more likely to operate in an eccentric way. In this situation, the dynamic characteristic and output

*Corresponding author: Tel: +8613437185849
Fax: +8602787859505, e-mail: wangnianxian1987@163.com

of the generator are unpredictable and the MWTG may not be able to work in practice; however, studies on the MWTG at present have not focused on this problem. Therefore, this problem becomes the key problem for the MWTG study, and needs to be addressed before the MWTG technology can be widely used.

In order to study the dynamic characteristic of the generator, a horizontal axial MWTG support with PMB is designed in this research; the 2D FEM model of magnetic flux and 3D FEM model of the rotor system have been constructed, and the radial force and rotor dynamic performance are analyzed in detail. Finally, the influence of PMB stiffness on the dynamic characteristic is indicated, and the stiffness design guideline for the MWTG is proposed.

2. Structure of MWTG

2.1. Structure of MWTG

A horizontal axial MWTG is designed. The rated power is 500W and the rated speed is 450r/min. The structure of the MWTG is shown in Fig. 1.

The MWTG has six primary components, including blades, a PMB, a shaft, a generator, a mechanical bearing, and an adjustment mechanism. The main radial load of the generator rotor is supported by the PMB in this MWTG. However, according to Earnshaw's law, the radial PMBs are unstable in the axial direction and the main benefit of the mechanical bearing is to keep the shaft stable. For the majority loads that are supported by PMB, the friction and the starting torque of the wind turbine generator are small; the efficiency of the drive train can therefore be improved and the maintenance cost can be reduced [8].

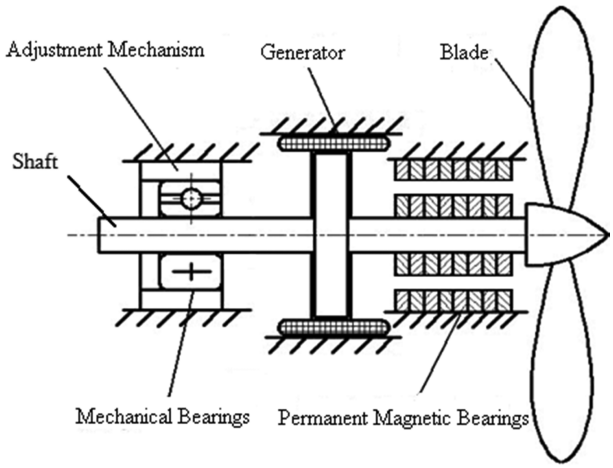

Fig. 1. Structure of MWTG.

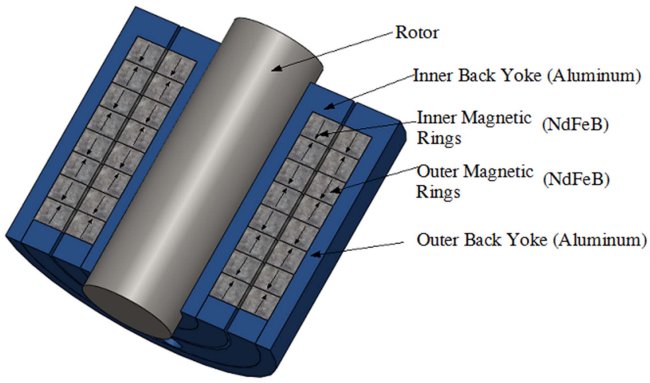

Fig. 2. (Color online) Structure of PMB.

2.2. Bearing capacity of PMB

The axial-magnetization and axial-position PMB have been used in this MWTG. The magnetizing and installation of these types of PMBs is easy [9]. The structure of the PMB after optimization is given in Fig. 2 and the directions of the arrows are the polarization direction of magnetic rings. In order to reduce the unwanted flux leakage and easily assemble the PMB, we use aluminum as the material of the back yoke, and the material of magnetic rings is NdFeB-45M.

The most important content in the PMB design is the bearing capacity design and the bearing stiffness design. The Coulombian model has been used in this research to calculate the bearing force [10, 11]. The magnetization model of the magnet ring is shown in Fig. 3. According to the magnetic charge model, magnetic charges are uniformly distributed on the polarization direction surface of the magnet rings, where the positive symbol refers to a positive magnetic charge and the negative symbol refers to a negative magnetic charge.

According to the Coulombian's law, the magnetic force between two magnetic charges is given in Eq. (1)

$$\vec{F} = \frac{1}{4\pi\mu_0} \cdot \frac{q_{m1} \cdot q_{m2}}{r^3} \cdot \vec{r} \tag{1}$$

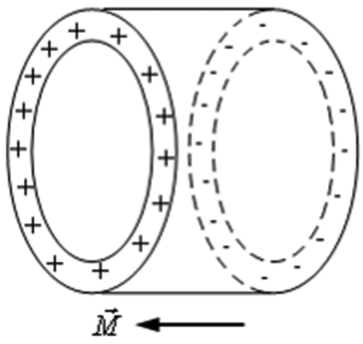

Fig. 3. Magnetization model of magnet ring.

where μ_0 is the magnetic permeability in the vacuum; $\vec{r}$ is the vector between magnetic charges; and q_{m1} and q_{m2} are the quantities of magnetic charges. Because the coercive force of NdFeB is large, the quantity of magnetic charges can be calculated using Eq. (2).

$$q_m = \mu_0 M = B_r \tag{2}$$

B_r is the residual magnetic flux density of the magnetic material.

Because both positive and negative magnetic charges are present, a repulsive force and an attraction force will occur between the magnetic charges.

In this study, the repulsive force has been designated asthe positive force, and the attraction force has been designated as the negative force.

The bearing force between the two magnetic rings can easily be calculated using Eq. (1). Usually, the bearing capacity of one pair of magnetic rings is small, and several pairs of magnetic rings will be used in the PMB to increase the bearing force. This research introduces the calculation of the bearing force of a PMB with 8 pairs of magnetic rings. The cross section of this PMB is shown in Fig. 4, and the parameters are given in Table 1.

In the Coulombian model, magnetic charges are distributed onthe surface of the magnet rings, and the magnet force mainly appears between the surface of the inner rings and outer rings. The surface numbers of the magnet rings are given in Fig. 4.

According to Eq. (1), the radial magnetic force between surface No. 1 and surface No. 10 is given as:

$$F_{1/10}=\frac{B_r^2}{4\pi\mu_0}\cdot\int_0^{2\pi}\int_0^{2\pi}\int_{R_{ii}}^{R_{io}}\int_{R_{oi}}^{R_{oo}}\frac{(e+r_1\cdot\sin\alpha-r_{10}\cdot\sin\beta)\cdot r_1\cdot r_{10}d\alpha d\beta dr_1 dr_{10}}{[a^2+(e+r_1\cdot\sin\alpha-r_{10}\cdot\sin\beta)^2+(r_1\cdot\cos\alpha-r_{10}\cdot\cos\beta)^2]^{3/2}} \tag{3}$$

The radial magnetic force between any two surfaces of inner rings and outer rings can be calculated:

$$F_{m/n}=\frac{B_{rm}\cdot B_{rn}}{4\pi\mu_0}\cdot\int_0^{2\pi}\int_0^{2\pi}\int_{R_{ii}}^{R_{io}}\int_{R_{oi}}^{R_{oo}}\frac{(e+r_m\cdot\sin\alpha-r_n\cdot\sin\beta)\cdot r_m\cdot r_n d\alpha d\beta dr_m dr_n}{[l_{mn}^2+(e+r_m\cdot\sin\alpha-r_n\cdot\sin\beta)^2+(r_m\cdot\cos\alpha-r_n\cdot\cos\beta)^2]^{3/2}} \tag{4}$$

where

$$\begin{cases} m=1,2,3\ldots 9 \\ n=10,11,12\ldots 18 \\ B_{rm}=B_r\ldots m=1,9 \\ B_{rm}=2B_r\ldots m=3,5,7 \\ B_{rm}=-2B_r\ldots m=2,4,6,8 \\ B_{rn}=B_r\ldots n=10,18 \\ B_{rn}=2B_r\ldots n=12,14,16 \\ B_{rn}=-2B_r\ldots n=11,13,15,17 \\ l_{mn}=a+|n-m-9|\cdot L \end{cases} \tag{5}$$

The bearing force of the magnetic bearing is the combination of radial magnetic forces. The bearing force and the bearing stiffness are given in Eq. (5) and Eq. (6), respectively:

$$F_p=\sum_{m=1}^{9}\sum_{n=10}^{18}F_{m/n} \tag{6}$$

$$K_p=\frac{dF_p}{de} \tag{7}$$

According to Eqs. (6) and (7), the bearing force and bearing stiffness of PMB have a relationship with the axial displacement and radial displacement, respectively. The bearing capacity cave of this PMB is given in Fig. 5.

In Fig. 5, (a) shows that the bearing force changed with different a and e, and (b) shows that the bearing stiffness changed with the different a. The influences of axial displacement on the bearing capacity are significant, and the axial displacement should be kept as small as possible.

Table 1. Parameters of cross section of the PMB.

Letter	Means	Value
a	axial displacement of rotor	
e	radial displacement of rotor	
L	length of magnet rings	12 mm
R_{ii}	inner radius of inner magnet rings	30.5 mm
R_{io}	outer radius of inner magnet rings	45.5 mm
R_{oi}	inner radius of outer magnet rings	47 mm
R_{oo}	outer radius of outer magnet rings	62 mm
B_r	residual magnetic flux density of magnet material	1.38T

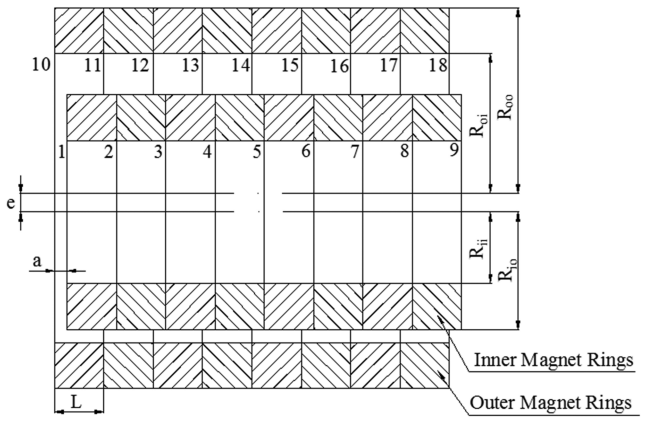

Fig. 4. Cross section of PMB.

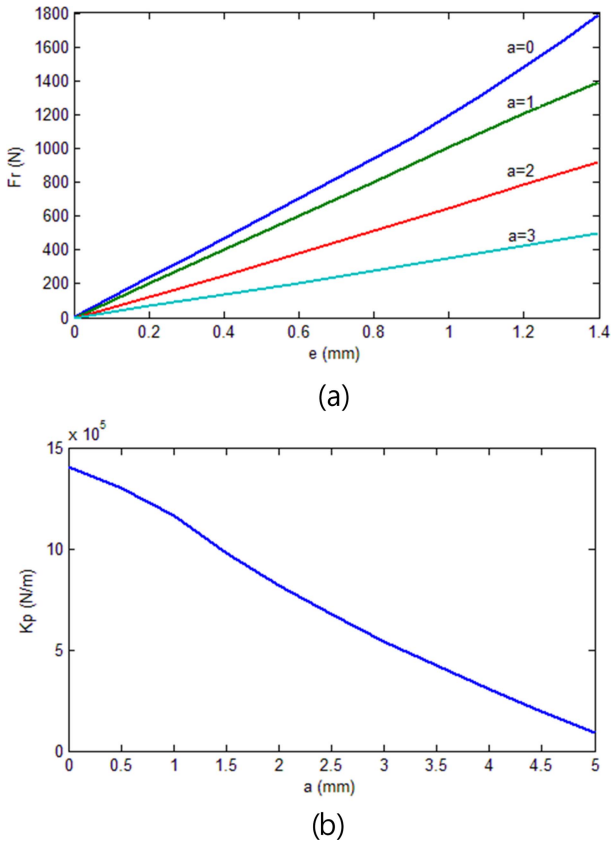

Fig. 5. (Color online) Bearing capacity cave of PMB.

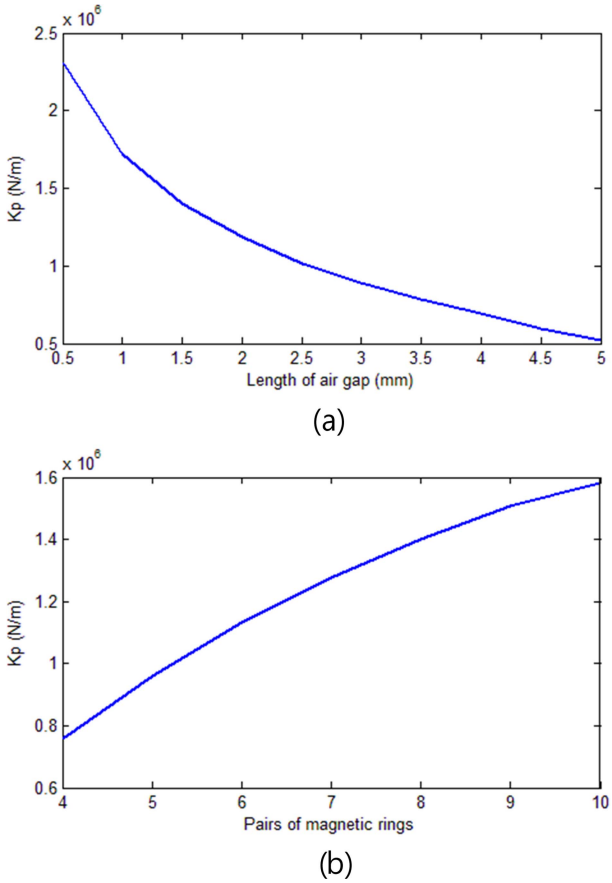

Fig. 6. (Color online) Bearing stiffness of PMB.

This is why the adjustment mechanism has been used in this MWTG. The bearing stiffness is determined by the axial displacement, and it is a constant value when a is constant. A radial displacement will occur when loading on the PMB; the radial displacement is a necessary condition, and it is defined by the load. Therefore, the rotor of the MWTG will work in an eccentric location during the operation.

Figure 5 shows the bearing stiffness of a PMB with 8 pairs of magnetic rings, and shows the influence of axial displacement of the rotor on the bearing stiffness. The axial displacement is not the only factor affecting the bearing stiffness; it can also be affected by the structure parameters of PMB, such as length of air gap, number of magnetic rings pairs, and dimension of magnetic rings etc.

In order to meet the requirement of the weight and dimensions of the MWTG structure in this research, R_{ii}, R_{oo}, and the total length of the PMB in Table 1 are restricted. Therefore, the length of air gap and number of magnetic rings pair become the two main factors that influence the bearing stiffness of the PMB in this research. The bearing stiffness of PMB with different numbers of magnetic rings and different air gaps when the PMB have the same R_{ii}, R_{oo} and the total length are given in Fig. 6.

Figure 6(a) shows the relationship between the length of air gap and bearing stiffness of 8 pairs of PMB magnetic rings, and (b) shows the relationship between the number of pairs of magnetic rings and the bearing stiffness when the length of air gap is 1.5 mm. It can be seen that the length of air gap and number of magnetic rings are very important in the stiffness design in PMBs. A different bearing stiffness can be obtained in the same sized spaces by using different lengths of air gap and different numbers of magnetic rings; the bearing stiffness variation range can also be significant.The bearing stiffness design of the PMB should meet the requirement of the MWTG.

3. Force analysis of MWTG

3.1. Radial force of rotor system

The generator in this MWTG is a permanent magnet generator. Radial forces on the rotor system are given in Fig. 7 and the meanings of the letters and values are given in Table 2.

The force balance equation is given in (8)

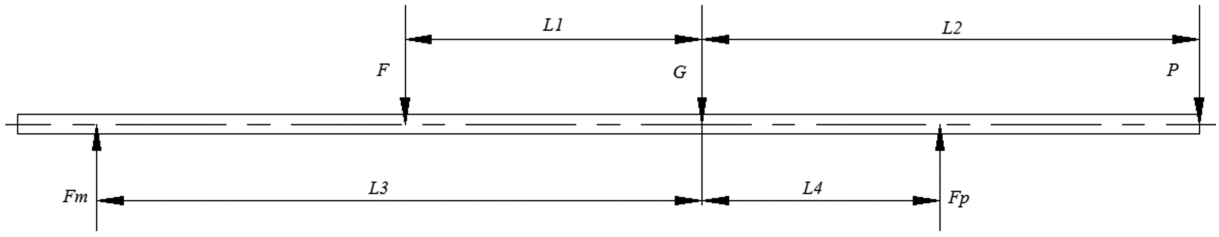

Fig. 7. Radial force on rotor system.

Table 2. Means of radial forces and values on the rotor system.

Letter	Means	Value
F_p	bearing force of PMB	
F_m	bearing force of mechanical bearing	
P	gravity of blades	112.7N
G	gravity of rotor system	103.55N
F	radial force caused by permanent magnets on generator rotor	
L_1	displacement between F and G	107 mm
L_2	displacement between P and G	176 mm
L_3	displacement between F_m and G	159 mm
L_4	displacement between F_p and G	41 mm

$$\begin{cases} F_m+F_p=P+G+F \\ F_m \cdot L_3 + P \cdot L_2 = F_p \cdot L_4 + F \cdot L_1 \end{cases} \quad (8)$$

Clearly, G and P are constant values, F_p, F_m, and F are unknown, and F_p and F_m are defined by F.

F is related to the magnetic flux distribution in the generator air gap, and it may differ during the operation. For the symmetrical structure of the generator, F is zero when the rotor center and the stator center are in the same position, and the situation will differ when the rotor has an eccentric displacement. According to the study, the rotor eccentricity will definitely occur during the operation in this MWGT, where F is a variable value. While the variation range of F has been discussed in [12], this research will study the frequency of F.

The radial force in the generator is the cause of the difference of MWTG dynamic performance. As the radial force is caused by the flux, this research analyzed the magnetic flux in the generator when the generator rotor has an eccentric displacement. The geometric parameters of the generator are given in Table 3.

The ANSYS result of flux in the generator is shown in Fig. 8, and the rotor eccentricity is generated in the x direction.

Given that the magnetic flux in the air gap is uniform in the radial direction, a circular path near the stator is defined, and the flux density of the air gap can be replaced by the flux density on the path. The magnetic flux density

Table 3. Geometric parameters of the generator.

Letter	Means	Value
S	eccentric displacement of generator rotor	
n	pole pair numbers	5
k	slot numbers	48
g	length of air gap	0.75 mm
R_r	diameter of rotor	74 mm
R_s	diameter of stator	210 mm
	material of permanent magnetic	NdFeB-45M
	material of stator	35w270

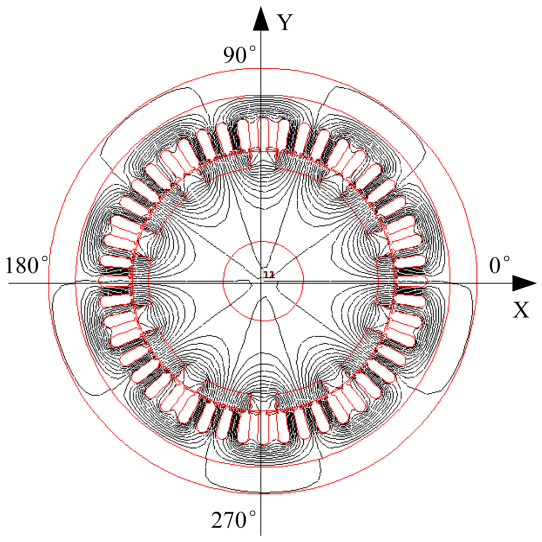

Fig. 8. (Color online) Magnetic flux in permanent magnet generator.

in the air gap when the rotor has an eccentric displacement is shown in Fig. 9 ($S = 0.5$ mm for example). In order to study the influence of rotor angle displacement (the mechanical angle of the rotor compared to the initial position is shown in Fig. 8 and a pair of magnetic poles are located in the X direction), the two curves in Fig. 9 indicate the different angle displacements of the generator rotor (angle displacements are 0 and 5 degrees).

According to Fig. 9, the flux amplitude near 0 degrees has increased to about 0.75T, and the flux amplitude near 180 degrees has decreased to about 0.6T; the magnetic

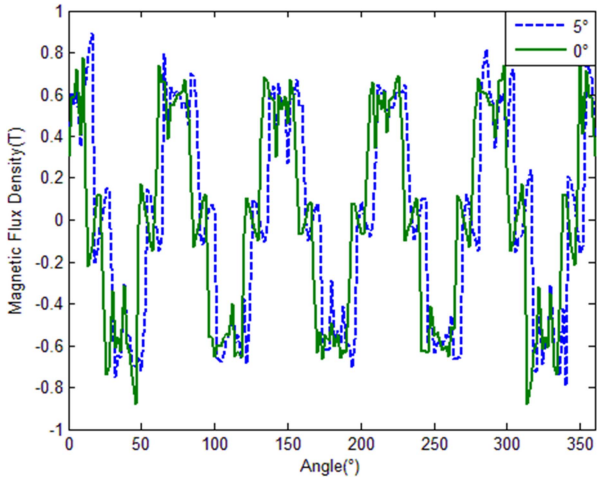

Fig. 9. (Color online) Magnetic flux density in air gap.

fluxes in the air gap become asymmetrical. Two conclusions can be drawn from this figure. Firstly, when the magnetic force is proportional to the square of the magnetic flux density, the radial magnetic force around the generator rotor will be asymmetrical and F will no longer be zero in the eccentric direction. Secondly, the distribution of the magnetic field changes with the angle displacement of the rotor; F will also change with the angle displacement of the rotor.

Owing to the small stiffness of PMB, S will change in a wide range when loading on the generator, and the characteristics of F need to be determined. In this research, the variation of F during no-load operation has been studied.

The radial forces of the generator rotor with different angle displacements and different eccentric displacements are shown in Fig. 10. For the case where the structure of

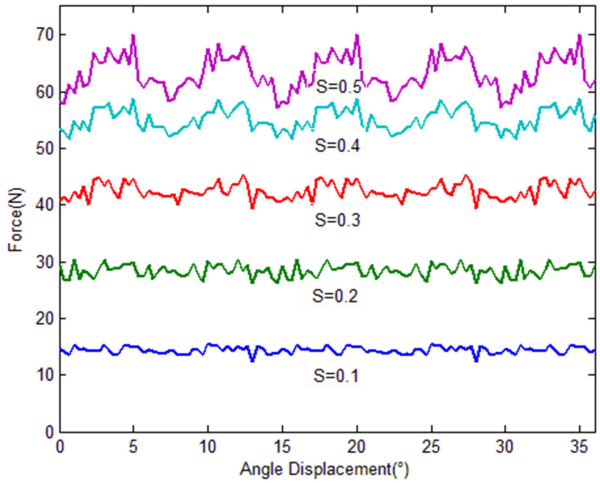

Fig. 10. (Color online) Radial force of generator rotor with different angle displacements.

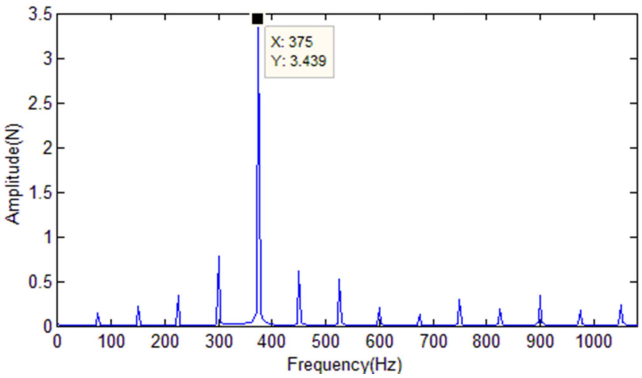

Fig. 11. (Color online) Frequency spectrum of radial force.

the generator is symmetrical, this study merely analyzes the smallest symmetrical part of the generator (36 degrees).

Figure 10 shows that F is significantly influenced by S, and a large value of S means F is also large. This could also indicate that harmonics appear in F, and that F changed in cyclical magnetic forcewith the increased angle displacement.

According to the structure of the MWTG and the operating characteristics of the PMB, F will affect the generator performance in two ways. Firstly, the shaft eccentric displacement will be affected. A larger value of F means a greater load on the PMB, and a larger eccentric displacement of the shaft. These influences have been discussed in [12]. Secondly, the vibration of the shaft will be affected. When F varies in the cyclical magnetic force, the shaft may work in the resonant frequency during the operation; in this research, F is examined in the frequency spectrums.

When the main frequency of F is determined by the number of slots/poles and the operation speed of the generator, the frequency spectrums of F under the rated speed during $S = 0.5$ mm is given in Fig. 11 (the frequency spectrums of F during other values of S are the same).

According to Fig. 11, the main frequency of F during the rated conditions is 375 Hz. The shaft will thus have a periodic force during operation in the rated condition, and the main frequency is 375 Hz.

4. Dynamics Analysis of MWTG

According to this study, a visible periodic force loading occurs on the rotor system of MWTG, and the frequency of the force is nearly constant. The dynamic characteristics of the rotor system need to be analyzed to avoid the resonance of the shaft.

The dynamic characteristic of the rotor system of MWTG is very complex, and excitation forces contain the magnetic

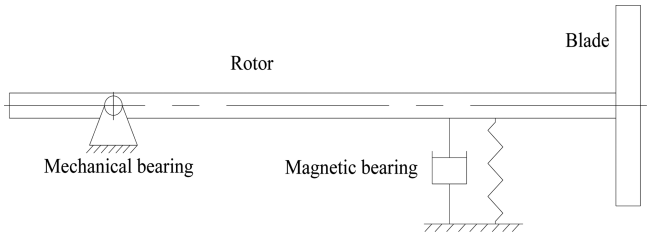

Fig. 12. Support model of rotor system.

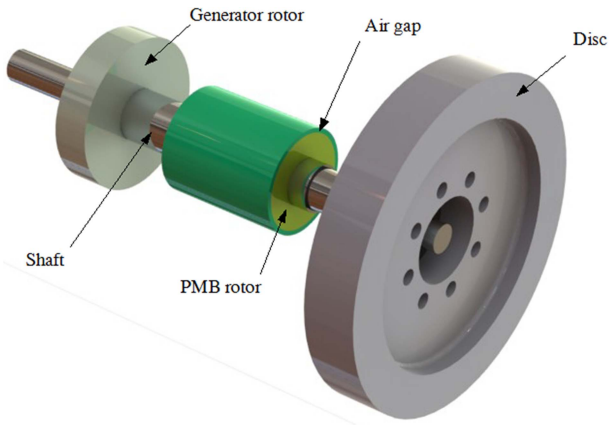

Fig. 13. (Color online) Structure of rotor system.

force and the wind load; analysis is therefore difficult. The main purpose of this research is to study the influence of the magnetic force in the generator, sothe influence of the blade has been ignored. The blades are replaced by the aluminum alloy disc, and the disc has the same weight and moment of inertiaas the blades.

In the MWTG, the bearing of the rotor system is produced by a mechanical bearing and a PMB. According to the bearing characteristics, the mechanical bearing can be simplified as a hinge structure, and the magnetic bearing can be simplified as a spring-damper system. The supporting model of the MWTG rotor system is shown in Fig. 12.

The structure and the FEM model of the rotor system are shown in Figs. 13 and 14.

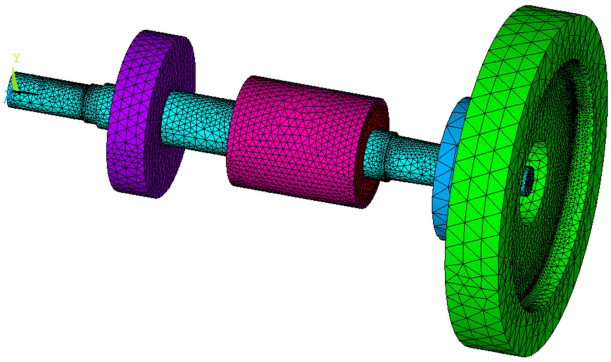

Fig. 14. (Color online) FEM model of rotor system.

Table 4. Material properties of rotor system components.

Components	Material Properties		
	Density (Kg/m^3)	Poisson's ratio	Young's modulus (Pa)
Shaft	7850	0.30	2.1e11
Generator rotor	2800	0.38	7.4e10
Disc	2800	0.38	7.4e10
PMB rotor	7500	0.29	1.7e10
Air ring	0	0	E

In order to simulate the spring-damper system, an air ring surrounding the PMB rotor was built as shown in Fig. 13, and the material properties of the air ring can be changed to obtain different bearing stiffnesses and dampers of PMB. The damper of the PMB is very small [1] and can be ignored in this research. Therefore, Young's modulus of the air ring is the only material property that needs to be defined, and the density and Poisson's ratio of the material property is set to zero. The material properties of the components ofthe rotor system are given in Table 4:

$$\text{where, } E = \frac{\sigma}{\varepsilon} = \frac{F}{S} \Big/ \frac{dl}{l} \tag{9}$$

S is the inner area of the air ring, $S = 3.43 \times 10^{-2} m^2$; l is the radial length of the air ring, and $l = 4.5 \times 10^{-3}$ m.

When the bearing capacity of this PMB is linear, the relationship between K_p and E can be obtained from Eqs. (7) and (9):

$$E = K_p \frac{1}{S} = 0.131 K_p \tag{10}$$

In the FEM analysis, displacement boundaries are used in the outside nodes of the air ring and the center of the mechanical bearing.

For example, several typical analysis results are given in Fig. 15 for when $K_p = 1 \times 10^3$ N/m.

In this research, the rigid mode and the first and second flexural modes of the rotor systemare analyzed for the case when the frequency of F is low. The modes of the rotor system analyzed using ANSYS are shown in Fig. 16.

Figure 16 shows the relationship between the mode frequencies of the rotor system and bearing stiffness. The increase of bearing stiffness can change the mode frequency, and the influences differ.

In Fig. 16, the first and second flexural mode frequencies are nearly stable when the bearing stiffness increased from 0 to 1×10^6 N/m, and these two mode frequencies are then increased linearly when the bearing stiffness increases from 1×10^6 to 2×10^7 N/m. However, the effect on the rigid mode frequency differs. With the increase of

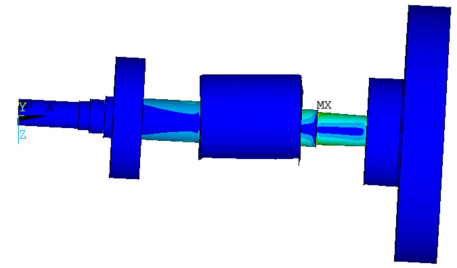

Rigid Mode (1.42Hz)

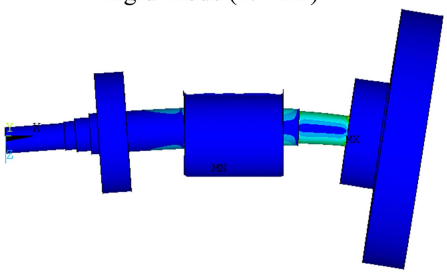

First Flexural Mode (280.38Hz)

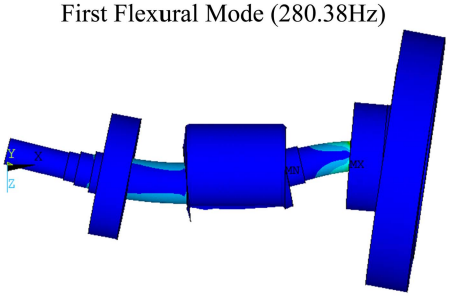

Second Flexural Mode (846Hz)

Fig. 15. (Color online) Mode shapes of rotor system.

bearing stiffness, the rigid mode frequency is increased significantly when the bearing stiffness is smaller than 1×10^6 N/m, and the mode frequency then becomes stable. The mode frequency increases to about 125 Hz when the bearing stiffness is 2×10^7 N/m. The rigid mode and the first flexural mode then become blended.

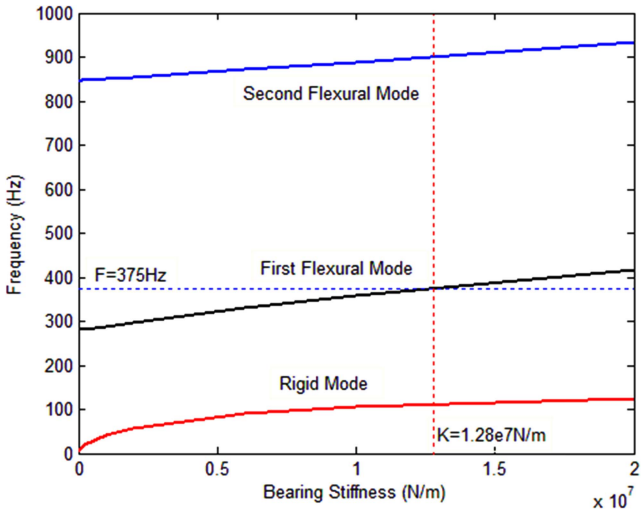

Fig. 16. (Color online) Modes of rotor system.

In the abovestudy, the main frequency of excitation force on the rotor system during the rated conditions is about 375 Hz, but the first flexural mode frequency of the rotor system can change from 280 Hz to 420 Hz. The rotor system will work in the first flexural mode when the bearing stiffness is close to 1.28×10^7 N/m and the system will become unstable. The main rule of the bearing stiffness design in the MWTG is to avoid this area.

5. Experiment

According to the FEM study, the mode frequencies of the rotor system in this research are remote from the main frequency of *F*, but the situation may differ in the real system for the machining error and assembling error.

The performance needs to be verified by experiment.

The test rig of the MWTG is shown in Fig. 17 and the inner magnetic rings and outer magnetic rings are shown in Fig. 18.

When the magnetic rings have an array of opposite magnetic poles, it is difficult to assemble these magnetic

Fig. 17. (Color online) Test rig of MWTG.

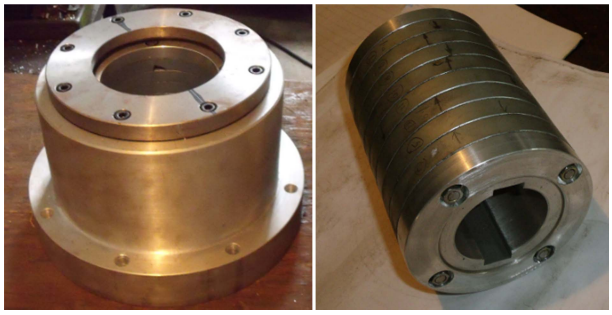

Fig. 18. (Color online) Outer magnetic rings and inner magnetic rings.

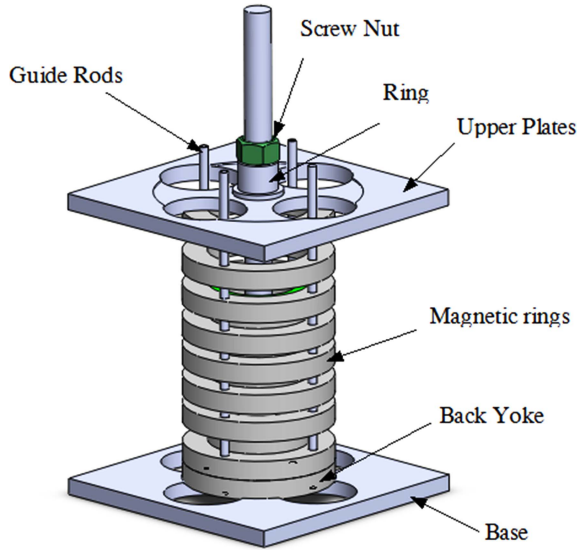

Fig. 19. (Color online) Structure of assembly instrument.

rings; an assembly instrument was thus designed in this study. The structure of the assembly instrument is shown in Fig. 19.

In this research, the design bearing stiffness of the PMB is 1.4×10^6 N/m (air gap is 1.5 mm and the number of magnetic ringspairs is 8). The rigid mode frequency of the rotor system is 49.9 Hz, the first flexural mode frequency is 292.17 Hz, and the second flexural mode frequency is 851.68 Hz. These frequencies are remote from the main frequency of *F*; theoretically, the MWTG will not work in the resonance area.

5.1. Experiment of PMB bearing capacity

Firstly, the bearing stiffness of the MWTG has been tested, and the experiment image is given in Fig. 20.

The force indicator and dial indicator were used in this experiment; the weights were loaded on the radial direction of the rotor system through the force indicator, and the radial displacements in this direction were simultaneously measured by the dial indicator. By loading gradually and reading the numbers on the force indicator and dial indicator, the bearing capacity curve of the rotor system can be obtained. The experiment result of the PMB bearing capacity curve is given in Fig. 21.

According to the experiment results, the bearing stiffness of this PMB is about 4.85×10^5 N/m, and is smaller than the theoretical value. The difference between the experiment result and the theoretical result may be fixed by the magnetization error and assembling error and this will be discussed in further research.

In this research, the bearing stiffnessis about 4.85×10^5, and the calculations of the rigid, first flexural, and second

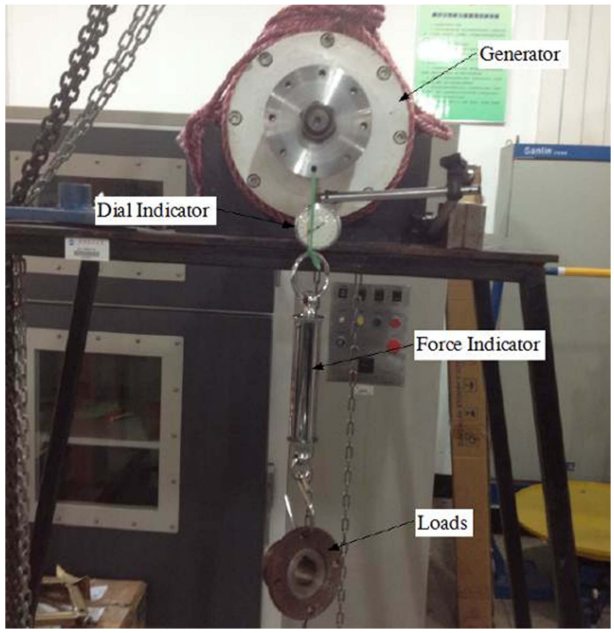

Fig. 20. (Color online) Experiment of PMB bearing capacity.

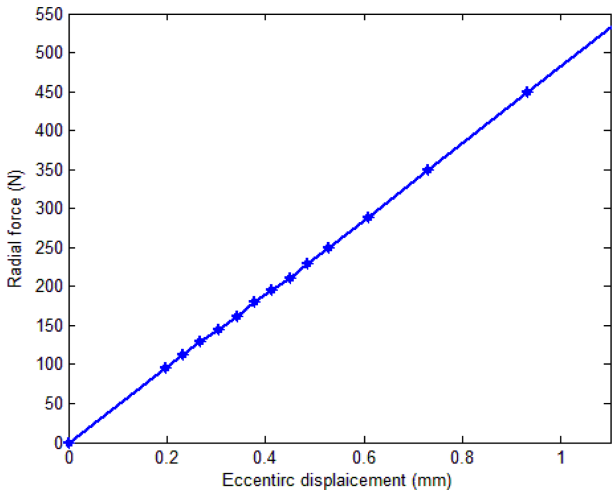

Fig. 21. (Color online) Bearing capacity curve of PMB in experiment.

flexural mode frequencies of the rotor system are 29.75 Hz, 284.48 Hz, and 847.97 Hz, respectively. These results differ from the design results and still significantly differ from the main frequency of *F*.

5.2. Experiment of natural frequency of the rotor system

The frequency characteristic of the rotor system was then tested by using the B&K system. The experiment is shown in Fig. 22.

Two acceleration sensors were used in this test, and the radial acceleration singles of the rotor system were

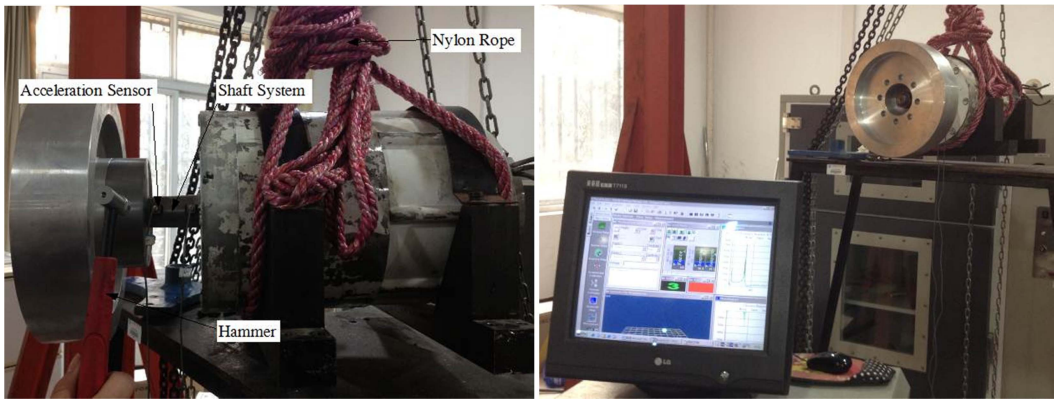

Fig. 22. (Color online) Experiment of natural frequency of the rotor system.

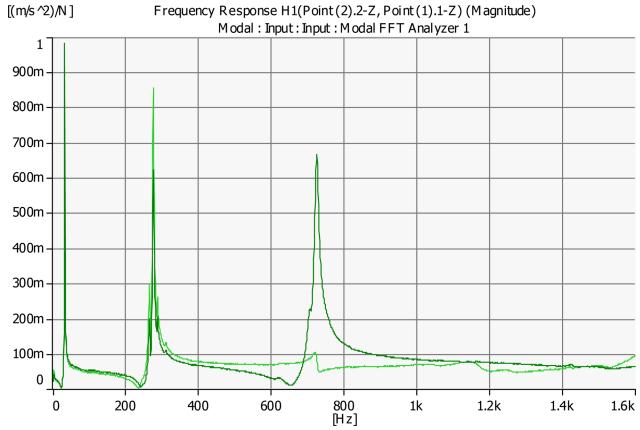

Fig. 23. (Color online) Test result of fequencycharacteristics of MWTG.

measured simultaneously. In this method, the error that occurred when the detect point was in the dead node can be avoided. The MWTG was hoisted by anylon rope to avoid the influence of the tower in the mode test. The fixed method and the hammer have been used to impel the rotor system in the measured direction.

The test area is from 0 Hz to 1.6K Hz, and the experiment result is shown in Fig. 23.

According to the test result, the front three nature frequencies of the rotor system are observed, and are 31 Hz, 274 Hz, and 724 Hz. The 31 Hz component is the rigid mode frequency of the system, the 274 Hz component is the first flexural mode frequency of the system, and the 724 Hz component is the second flexural mode frequency of the system.

Compared with the theoretical results, the rigid mode frequency and the first flexural frequency are closed, but the second flexural mode frequency is smaller than the theoretical result.

The main reason for this might bebecause, while the analysis model of the rotor system should be integrated, the rotor system has several parts, including the shaft, the generator rotor, and the PMB rotor. All these parts are installed in the shaft and the amount of interference is very small, so the analyzed flexural mode frequency is larger than the test result. The analysis results are rational in this study.

According to the results, the natural frequencies of the rotor system are remote from the main frequency of F.

The shaft will not work in the resonance area. Therefore, the MWTG can operate stably during the rated conditions, even when it has a shaft eccentric displacement.

6. Conclusions

In this paper, a horizontal axial MWTG supported with a permanent magnetic bearing (PMB) was designed. The 2D FEM model of the magnetic flux and the 3D FEM model of the rotor system were constructed and the radial force and the influence of bearing stiffness in MWTG were studied.

The result shows that the eccentric displacement is the necessary condition in this type of MWTG, and the performance of MWTG will be affected. In the eccentric position, gravities are not the only radial loads on the rotor system; a cyclical magnetic force will occur between the rotor and stator in the generator. This force will affect the generator performance in two ways: in the shaft eccentric displacement and in the vibration of the rotor system. The research shows that a larger value of radial magnetic force means a greater value of eccentric displacement, and the frequency of the radial magnetic force is nearly constant during the rated operation.

The dynamics of the rotor system were also studied. The result shows that the mode frequency of the rotor system will be affected by the bearing stiffness, and the

natural mode may be located near the main frequency of the magnetic force. The bearing stiffness design needs to avoid the resonance area. This is the main rule of the bearing stiffness design in the MWTG.

The rule can also be used in other maglev permanent magnet motors.

Acknowledgments

This work was supported by the Natural Science Foundation of China (No. 51175390).

References

[1] Y. Hu, Z. Zhou, and Z. Jiang, Basic Theory and Application of Active Magnetic Bearing, China Machine Press (2006).
[2] G. Shrestha, H. Polinder, D. J. Bang, and J. A. Ferreira, IEEE Tran. Energy Conversion, **25**, 732 (2010).
[3] G. Shrestha, H. Polinder, D. J. Bang, and J. A. Ferreira, Proceedings Offshore wind 2007 (2007).
[4] N. C. Tsai and C. W. Chiang, Mechanical Systems and Signal Processing, **24**, 873 (2010).
[5] H. Wu, L. Xiao, B. Wang, G. Li, and P. Li, Proceedings of 2010 IEEE/ASME, International Conference on Mechatronic and Embedded Systems and Applications (2010) pp. 283-287.
[6] S. Liu, Z. Bian, D. Li, and W. Zhao, Asia-Pacific Power and Energy Engineering Conference (2010).
[7] Y. H. Fan, Y. T. Lee, C. C. Wang, and Y. L. Liao, Appl. Mechanics and Materials, **145**, 174 (2012).
[8] N. Wang, J. Zhang, and Y. Hu, Journal of Wuhan University of Technology (information& management engineering), **36**, 896 (2010).
[9] B. Paden, N. Groom, and J. F. Antaki, J. Mech. Des., **125**, 734 (2003).
[10] R. Ravaud, G. Lemarquand, and V. Lemarquand, IEEE Trans. Magn., **45**, 2996 (2009).
[11] R. Ravaud, G. Lemarquand, and V. Lemarquand, IEEE Trans. Magn., **45**, 3334 (2009).
[12] N. X. Wang, J. G. Zhang, and G. P. Ding, Appl. Mechanics and Materials, **105**, 57 (2012).
[13] W. J. Yu and X. Y. Qian, Appl. Mechanics and Materials, **195**, 47 (2012).